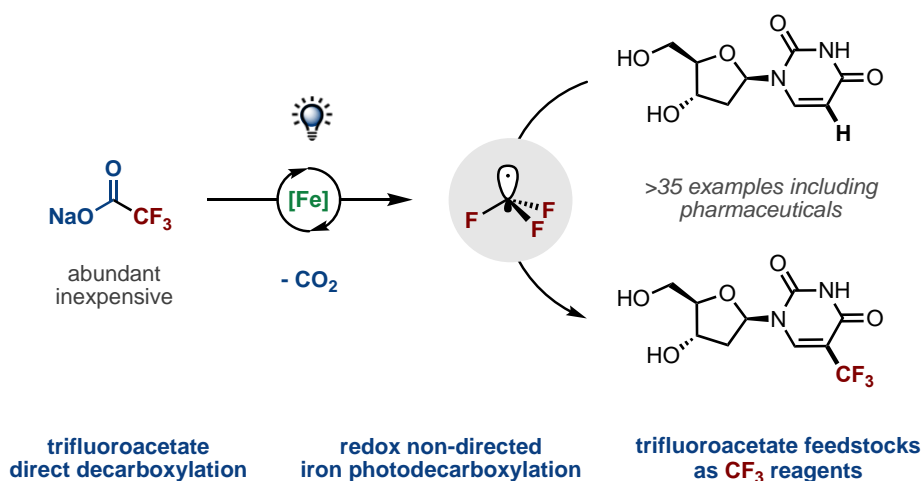# Direct Decarboxylation of Trifluoroacetates Enabled by Iron Photocatalysis

Sara Fernández-García, Veronika O. Chantzakou, Francisco Juliá-Hernández*

Departamento de Química Inorgánica, Facultad de Química, Universidad de Murcia, Campus de Espinardo, 30100 Murcia, Spain.

Corresponding autor: francisco.julia@um.es

ABSTRACT.

Trifluoroacetates are the most abundant and accessible sources of trifluoromethyl groups, which are key components in pharmaceuticals and agrochemicals. The generation of trifluoromethyl reactive radicals from trifluoroacetates requires their decarboxylation, which is hampered by their high oxidation potential. This constitutes a major challenge for redox-based methods, because of the need to pair the redox potentials with trifluoroacetate. Here we report a strategy based on iron photocatalysis to promote the direct photodecarboxylation of trifluoroacetates that displays reactivity features that escape from redox limitations. Our synthetic design has enabled the use of trifluoroacetates for the trifluoromethylation of more easily oxidizable organic substrates, offering new opportunities for late-stage derivatization campaigns using chemical feedstocks, Earth-abundant catalysts, and visible-light.

1

MAIN TEXT.

Synthetic organic chemistry has adopted photocatalytic methods because they facilitate the formation of reactive radical intermediates, leading to attractive methodologies fueled by visible-light illumination.[1–3] Photoredox catalysis enables the generation of these species via a photoinduced single-electron transfer (SET), capitalizing the improved redox properties of excited-state photocatalysts compared to those in the ground state.[4] This approach has been used to expedite the decarboxylation of carboxylic acids,[5] motifs existing in abundant materials and industrially relevant molecules. Upon visible-light absorption, the excited-state photocatalyst promotes single-electron oxidation of the carboxylate conjugate base, which generates a carboxylate radical that rapidly extrudes CO_2 (Figure 1A). The resulting C-centered radical is amenable to subsequent bond-forming reactions.[6] SET takes place via an outer-sphere pathway similar to ground-state redox reactions.[7] Due to the inherent nature of this event, the photoredox decarboxylation chemical space is delimited by two intrinsic hurdles: 1) Reactivity is governed by a match between redox potentials of both carboxylate and excited-state photocatalyst $[E_{ox}(RCO_2^-)<E(PC*/PC^-)]$ (Rehm-Weller thermodynamics).[8] 2) Redox potentials also influence electron transfer selectivity to some extent,[9] which results in the compound with the lowest oxidation potential often oxidizing more readily. In view of this, the decarboxylation of substrates with very high oxidation potentials while overcoming the redox-directed site-selectivity is currently a daunting scenario in photoredox catalysis.

Clear evidence of this challenge is the arduous direct photodecarboxylation of trifluoroacetate salts (Figure 1B). Trifluoroacetic acid is a chemical feedstock that is considered the most abundant and accessible source of trifluoromethyl groups (CF_3).[10] The incorporation of trifluoromethyl groups into organic molecules is a pivotal transformation in drug discovery and development campaigns, because it improves their biological activity.[11,12] Therefore, the effective use of inexpensive and atom-economical trifluoroacetates as trifluoromethyl radical sources, mostly dominated by expensive reagents with high enthalpic driving forces or toxic compounds,[13] would constitute a significant advancement. However, the utilization of trifluoroacetates as a CF_3 reagent in the trifluoromethylation of high molecular complexity substrates is currently hampered by the very high oxidation potential of trifluoroacetate salts (+2.4 V vs SCE in MeCN),[14] which has resulted in methodologies with harsh reaction conditions using strong oxidants (XeF_2)[15] and highly oxidizing electrochemical conditions,[14] with limited applicability. Additionally, its slower decarboxylation rate (10^5 s^{-1})[16] compared to other aliphatic carboxylic acids (10^8-10^9 s^{-1})[17] enables undesired back electron transfer processes (BET, Figure 1B). Despite these challenges, the synthetic utility of trifluoroacetates and its surrogates have been pursued with great effort in the past years,[18] notably with the use of Cu[19–21] and Ag[22] salts via

transition-metal-mediated and catalyzed decarboxylations that invariably occurred at elevated temperatures.[23] In sharp contrast to non-fluorinated aliphatic carboxylates, the direct photodecarboxylation of trifluoroacetates is currently beyond the scope of homogeneous photoredox catalysis,[24–26] due to the impossibility to match such high oxidation potential with a slow decarboxylation rate. This has led to the design of alternative undirected strategies involving its preactivation in the form of redox-active functionalities,[27–29] resulting in poor atom economy.
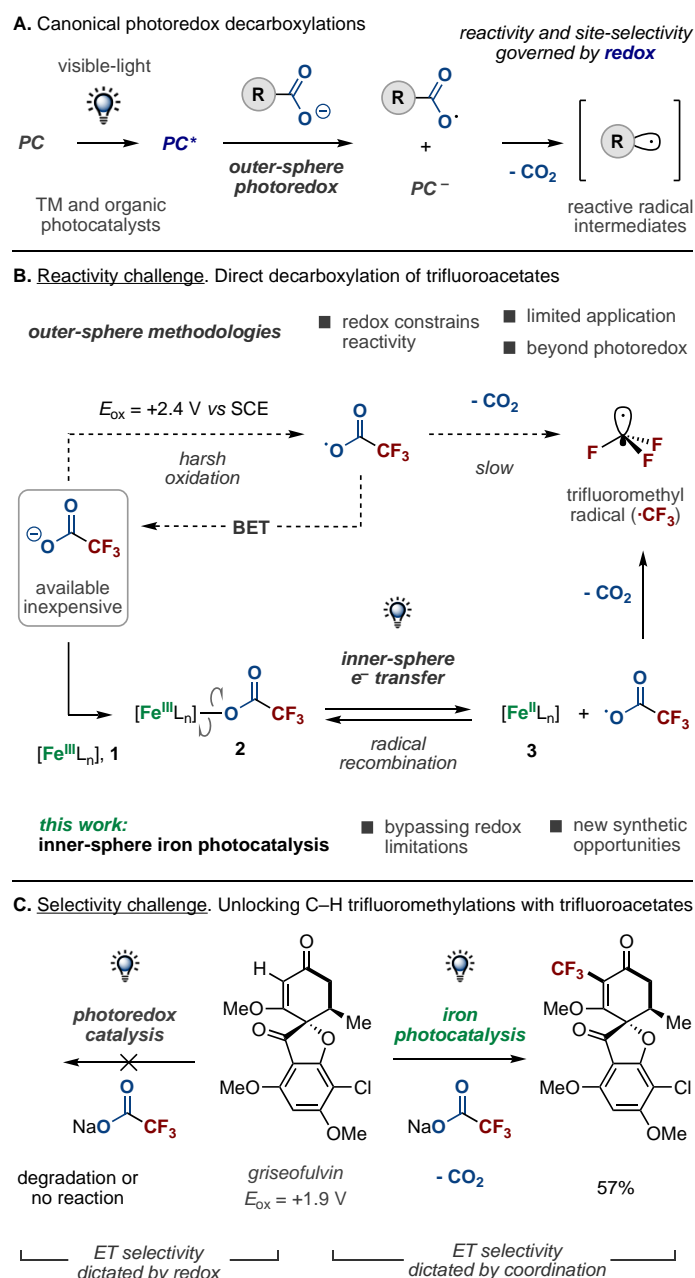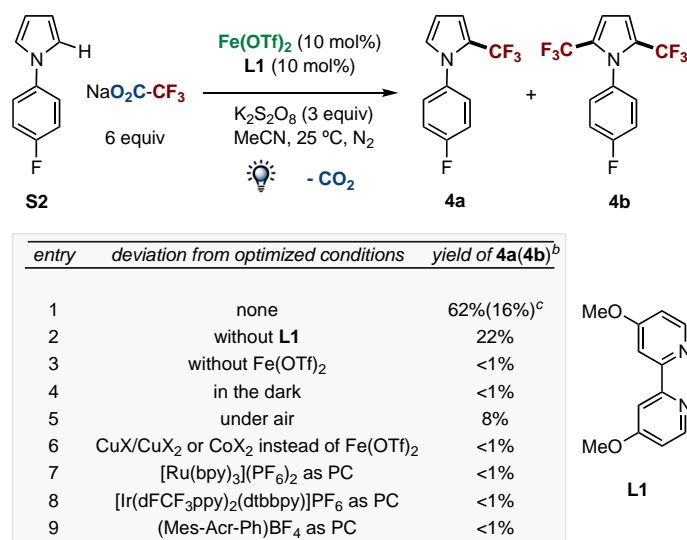

Figure 1. (**A**) Decarboxylations via photoredox catalysis. (**B**) Iron photocatalysis tackles the challenge of the direct decarboxylation of trifluoroacetates. (**C**) Trifluoromethylation reactions with trifluoroacetates enabled by iron photocatalysis. *ET* = electron transfer.

3

In this communication, we present the design of an iron photocatalyst that functions via a complementary inner-sphere electron transfer pathway, which bypasses the thermodynamic redox limitations of photoredox catalysts. This involves the coordination of trifluoroacetate to the Fe(III) active species (**1**, Figure 1B), which results in the formation of a Fe(III) carboxylate complex (**2**). Visible-light absorption triggers a Fe–O homolytic cleavage leading to Fe(II) species (**3**) and trifluoroacetate radical that decarboxylates to $^{\cdot}CF_3$. This process affords the products of a formal SET oxidation of trifluoroacetate with Fe(III) but without the existence of a bimolecular redox reaction. If radical recombination occurs prior to decarboxylation, it will directly regenerate **2** within the solvent cage, unlike undesired photoredox BET processes involving diffusion of species. Inner-sphere electron transfer arises from the population of a dissociative ligand-to-metal charge transfer (LMCT) excited state, an emerging concept in organic synthesis with Earth-abundant metals,[30,31] rooted in fundamental studies in the past.[32,33] Complementary LMCT decarboxylation strategies of non-fluorinated carboxylates with more accessible oxidation potentials have been recently reported with first-row transition metals[34–43] and cerium salts,[44–46] which have displayed similar or competing reactivity patterns to traditional photoredox catalysts. Yet, the full potential of LMCT photocatalysis in organic synthesis, such as the activation of substrates beyond redox demands, is to be unveiled.

We have applied our decarboxylation technology to the trifluoromethylation of $C(sp^2)$–H bonds in organic substrates. Thanks to the mode of action of our design, we have been able to tackle the selectivity challenge of promoting the direct decarboxylation of sodium trifluoroacetate (+2.4 V *vs* SCE) in the presence of substrates with much lower oxidation potentials (Figure 1C, right). This has allowed us to introduce CF_3 groups to various electron-rich (hetero)aromatics and pharmaceuticals like griseofulvin (E_{ox} = +1.9 V *vs* SCE),[47] without the interference of undesired bimolecular redox processes. This is virtually unattainable under photoredox settings, in which selectivity is at the mercy of redox thermodynamics, resulting in no reaction or degradation of the substrates (Figure 1C, left).

Our investigations to optimize the photocatalytic trifluoromethylation of $C(sp^2)$–H bonds gave rise to the conditions shown in Table 1.[47] The combination of Fe(OTf)$_2$ and 4,4'-dimethoxy-2,2'-bipyridine (**L1**) resulted in an active catalyst able to promote the decarboxylation of sodium trifluoroacetate (NaO$_2$CCF$_3$) and the trifluoromethylation of 1-(4-fluorophenyl)-1*H*-pyrrole (**S2**) with K$_2$S$_2$O$_8$ as oxidant at 25ºC under 405 nm illumination. The corresponding trifluoromethylated products **4a** and **4b** were formed in 62% and 16% yield, respectively (Table 1, entry 1). Control experiments demonstrated the photocatalytic activity of the iron species. Although a 22% yield of **4a** was obtained without **L1** (entry 2), no reaction was detected in the absence of iron salt or in the dark (entries 3-4). Trifluoromethylation was not detected when using cobalt or copper salts instead of iron

4

(entry 6),[47] which excludes the activity of traces of these metals as contaminants. For further comparison, no reaction or degradation of the substrate was observed when using Ru, Ir or, organic photoredox catalysts (entries 7-9). The oxidant is pivotal for the turnover of Fe(II) into catalytically active Fe(III) species, but it does not participate in the decarboxylation step (see mechanistic investigation). Other inorganic oxidants were productive, as well as other iron salts including $Fe(NO_3)_3 \cdot 9H_2O$.[47]

entry	deviation from optimized conditions	yield of 4a(4b)[b]
1	none	62%(16%)[c]
2	without L1	22%
3	without Fe(OTf)$_2$	<1%
4	in the dark	<1%
5	under air	8%
6	CuX/CuX$_2$ or CoX$_2$ instead of Fe(OTf)$_2$	<1%
7	[Ru(bpy)$_3$](PF$_6$)$_2$ as PC	<1%
8	[Ir(dFCF$_3$ppy)$_2$(dtbbpy)]PF$_6$ as PC	<1%
9	(Mes-Acr-Ph)BF$_4$ as PC	<1%

Table 1. Optimization of the trifluoromethylation of (hetero)arenes using trifluoroacetates[a]
[a]Reactions were performed with 0.3 mmol of **S2**. [b]Yields were determined by ^{19}F NMR using hexafluorobenzene as internal standard. [c]Isolated yield, 0.5 mmol of **S2**.

5

After optimization, we explored the substrate scope of the decarboxylative trifluoromethylation protocol (Table 2). A range of pyrroles with different substitution patterns at the aromatic nitrogen was found to produce the corresponding trifluoromethylated products in good yields, including aromatic (**4-6**), aliphatic (**7**, **9-11**) and, *N*-protecting groups (**8**). The poor solubility of $K_2S_2O_8$ in pure MeCN ensures mild oxidizing conditions. As expected, trifluoromethyl radical addition occurred at the C2 position.[48] In substrates bearing multiple reactive positions, bis-trifluoromethylated products were obtained like other reported radical trifluoromethylation reactions.[48] Substitution in the aromatic ring was also well tolerated, without observing degradation of aromatic halides (**4**, **6**) or undesired oxidation of aldehydes (**14**). Other 5-membered heteroaromatics (**15-16**), 6-membered heterocycles (**17-20**) and arenes (**21-23**) were also functionalized. It is worth noting that the catalyst was active in the presence of substrates bearing potentially coordinating N atoms, such as pyridines (**17**) and pyrimidines (**18**). A variety of differently substituted indoles were submitted to the reaction conditions, because of the presence of this motif in a broad collection of pharmacophores.[49] As expected, in most cases, mono- and bis-trifluoromethylated isomers were isolated (**24-27**), due to the presence of various reactive positions in their backbone.[50] The structure of the bis-trifluoromethylated compound **27c** was assigned by X-ray diffraction. Additionally, our protocol allowed the direct trifluoromethylation of ferrocene (**28**), which is an elusive transformation in the literature,[50,51] presumably due to the accessible oxidation to ferrocenium (+0.77 V). This highlights the ability of our synthetic design to circumvent undesired bimolecular redox processes.

6
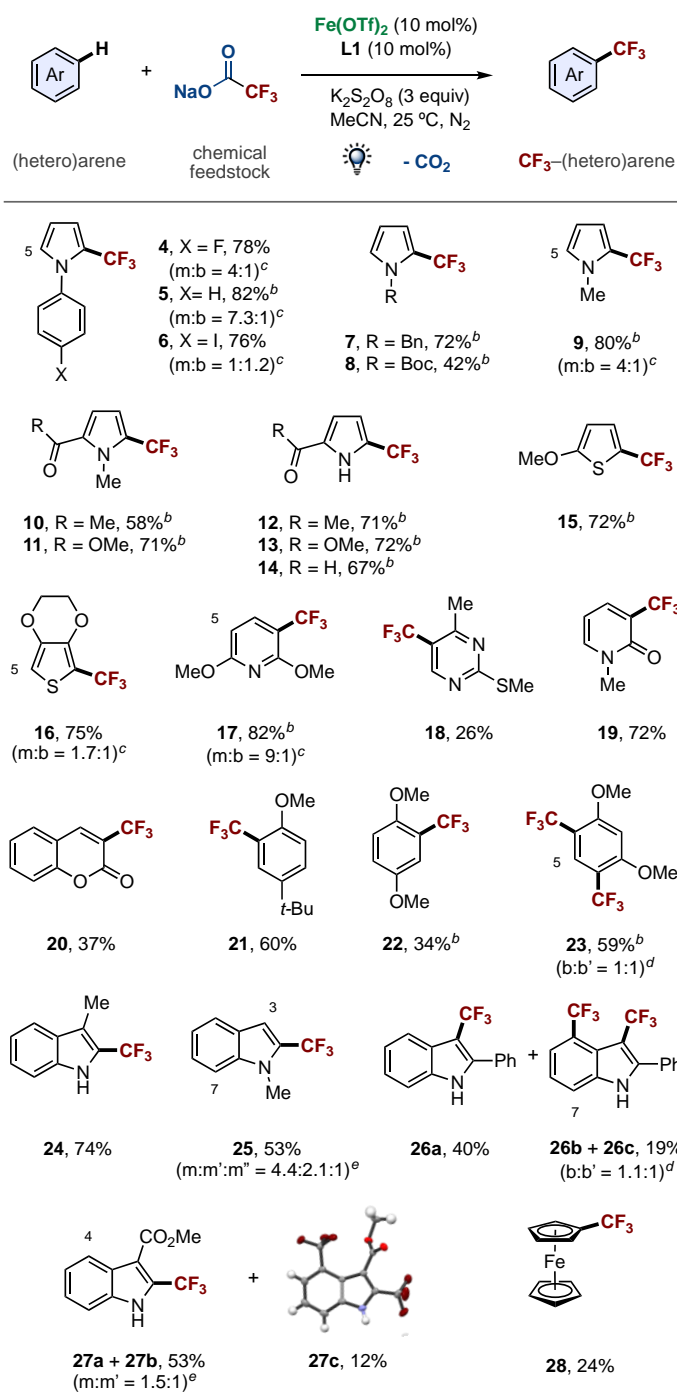
Table 2. Scope of the trifluoromethylation of C–H bonds with trifluoroacetates[a]

[a]Conditions: (Hetero)arene (0.5 mmol), NaO_2CCF_3 (4-6 equiv.), $Fe(OTf)_2$ (10 mol%), **L1** (10 mol%), $K_2S_2O_8$ (3 equiv.), acetonitrile (0.1 M), 405 nm irradiation, 25 ºC, 24-48 h. Isolated yields. [b]Yield determined by ^{19}F NMR using hexafluorobenzene as internal standard due to volatility of the product. [c]Ratio between mono (m) and bis-trifluoromethylated (b) products. [d]Ratio bis-trifluoromethylated isomers. [e]Ratio mono-trifluoromethylated isomers. Minor regioisomeric position labelled with atom number.

To further highlight the utility of our method, we submitted a collection of complex molecules including natural products, pharmaceuticals, and agrochemicals to our reaction conditions (Table 3). Generally, the incorporation of the trifluoromethyl group occurred at the most electron-rich $C(sp^2)$–H bond, presumably because of a polarity match with the rather electron-poor CF_3 radical.[52–54] This is a competent strategy to prevent metabolic degradation at high electron density reactive sites of biologically active compounds.[11] When caffeine, theophylline and pentoxifylline were tested under the optimized conditions, the corresponding trifluoromethylated products **29-31** were obtained in good yields. Protected and unprotected pyrimidine nucleobases also worked well (**32-34**), posing no inhibition problems to the catalyst. It is worth remarking that we were able to prepare trifluridine (Lonsurf®), one of the largest-selling small molecule pharmaceuticals,[12] in one step from unprotected 2-deoxyuridine in 61% yield (**33**). The antifungal griseofulvin (Gris-PEG®) and the muscle relaxant metaxalone (Skelaxin®) were trifluoromethylated at the olefinic enone and the aromatic ring, respectively, resulting in previously unreported **35** and **36**. A comparison of our protocol to other methods using trifluoroacetic acid and derivatives is shown in Table S6.[45] When the naturally occurring furanochromone visnagin was tested under reaction conditions, mono- (**37a**) and bis-trifluoromethylated (**37b**) derivatives were obtained. The trifluoromethylation of the nonsteroidal anti-inflammatory drug indometacin (Indocid®) and the natural product melatonin resulted in the formation of isomeric mono- (**38a**, **38b**), bis- (**39a**, **39b**) and even tris-trifluoromethylated products (**39c**, **39d**) because of their various reactive sites at the indole ring. Our method provides rapid access to multiple isolable trifluoromethylated isomers that could be of interest in hit-to-lead drug discovery programs.[48,55]
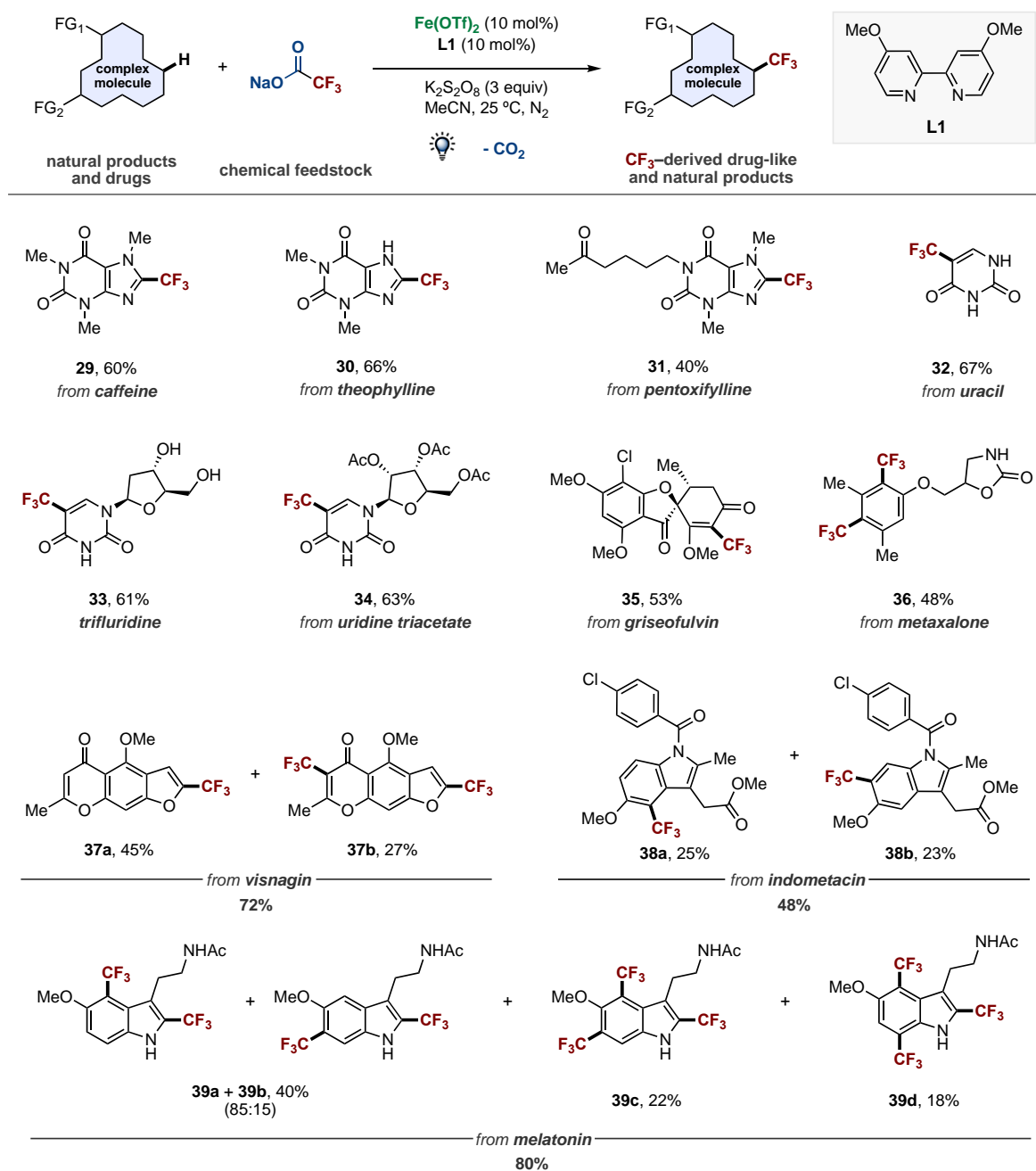
Table 3. Late-stage trifluoromethylation of natural products and drug-like molecules[a]

[a]Conditions: Substrate (0.5 mmol), NaO₂CCF₃ (6 equiv.), Fe(OTf)₂ (10 mol%), **L1** (10 mol%), K₂S₂O₈ (3 equiv.), acetonitrile (0.1 M), 405 nm irradiation, 25 ºC, 48 h. Isolated yields.

According to our research hypothesis, recent literature insights[40,41] and our experimental data, we propose the mechanistic pathway depicted in Scheme 1A. Initially, the catalytically active Fe(III) species (**1**) are formed *via in situ* coordination of **L1** to Fe(OTf)$_2$ and subsequent oxidation with K$_2$S$_2$O$_8$. Coordination of trifluoroacetate sets the stage for the inner-sphere photodecarboxylation with 405 nm illumination via Fe–O homolytic cleavage in **2**, resulting in the formation of $^\cdot$CF$_3$. This adds into the substrate, ultimately leading to the trifluoromethylated product after oxidation and rearomatization. Catalyst turnover is achieved by Fe(II) (**3**) to Fe(III) (**1**) oxidation with K$_2$S$_2$O$_8$. This mechanistic proposal is supported by experimental data for each of the elementary steps of the catalytic cycle. To begin with, the intermediacy of CF$_3$ radicals was supported by radical trap experiments (Scheme 1B). The addition of TEMPO ((2,2,6,6-tetramethylpiperidin-1-yl)oxyl) quenched the photodecarboxylation and afforded the TEMPO-adduct **40**; while the reaction with 1,1-diphenylethylene gave rise to the CF$_3$-incorporated product **41**. The key step involving the photodecarboxylation of trifluoroacetate from **2** was studied by UV-Vis spectroscopy. In the absence of oxidant, intermediate **2** (Scheme 1C, green trace), generated *in situ* by mixing Fe(NO$_3$)$_3$·9H$_2$O, **L1** and NaO$_2$CCF$_3$, evolved upon irradiation (purple trace) in the presence of **S2** to the formation of Fe(II) species (red trace). This process also yielded 60% of the trifluoromethylated product **4a**, calculated related to the amount of iron.[47] This demonstrates that photodecarboxylation occurs in the absence of an oxidant, which must be only responsible for rearomatization and catalyst turnover. The latter has been also confirmed by monitoring the oxidation of Fe(II) to Fe(III) with K$_2$S$_2$O$_8$ by UV-Vis spectroscopy.[47] Although preliminary, this mechanistic interrogation offers experimental evidence for the inner-sphere character of the photodecarboxylation reaction.

10
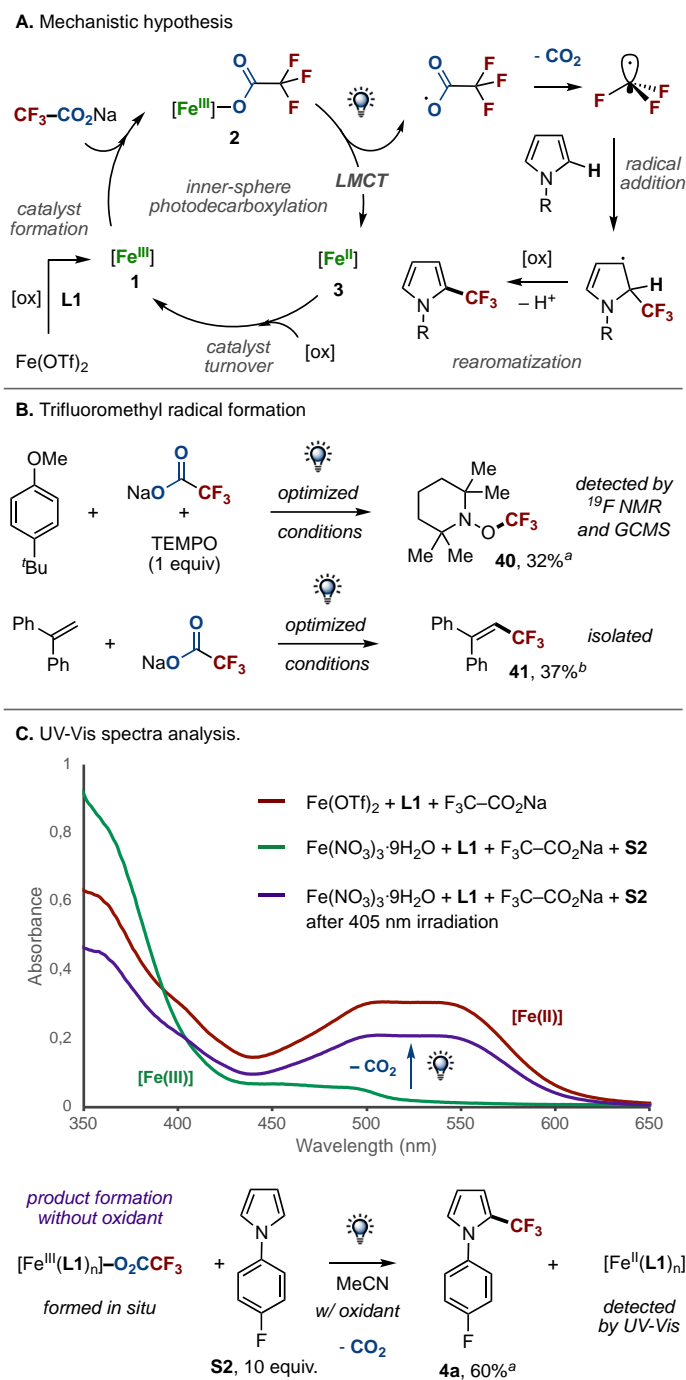
Scheme 1. (A) Proposed reaction mechanism. (B) Radical trap addition experiments. (C) UV-Vis analysis of the photodecarboxylation step
[a]Yields determined by ^{19}F NMR using hexafluorobenzene as internal standard. [b]Isolated yields.

Overall, in this report, we have described a photocatalytic system based on an Earth-abundant metal capable of expanding the scope of photodecarboxylation reactions by circumventing the necessity to pair redox potentials as it occurs in photoredox catalysis. We have enabled the opportunity of repurposing inexpensive trifluoroacetates in the $C(sp^2)$–H trifluoromethylation of organic substrates with much lower oxidation potentials, without observing redox degradations. The diversity of structural motifs and substituents showcased in the late-stage derivatization of complex molecules hold great promise for the exploitation of trifluoroacetates and other carboxylic acid feedstocks that are beyond the scope of photoredox catalysis, in the pharmaceutical and agrochemical sectors. We hope our study could set the stage for the discovery of new reactivity platforms to further uncover the synthetic potential of LMCT photocatalysis.

REFERENCES.

(1)   Crespi, S.; Fagnoni, M. Generation of Alkyl Radicals: From the Tyranny of Tin to the Photon Democracy. *Chem. Rev.* **2020**, *120* (17), 9790–9833. https://doi.org/10.1021/acs.chemrev.0c00278.

(2)   Juliá, F.; Constantin, T.; Leonori, D. Applications of Halogen-Atom Transfer (XAT) for the Generation of Carbon Radicals in Synthetic Photochemistry and Photocatalysis. *Chem. Rev.* **2022**, *122* (2), 2292–2352. https://doi.org/10.1021/acs.chemrev.1c00558.

(3)   Holmberg-Douglas, N.; Nicewicz, D. A. Photoredox-Catalyzed C–H Functionalization Reactions. *Chem. Rev.* **2022**, *122* (2), 1925–2016. https://doi.org/10.1021/acs.chemrev.1c00311.

(4)   Prier, C. K.; Rankic, D. A.; MacMillan, D. W. C. Visible Light Photoredox Catalysis with Transition Metal Complexes: Applications in Organic Synthesis. *Chem. Rev.* **2013**, *113* (7), 5322–5363. https://doi.org/10.1021/cr300503r.

(5)   Schwarz, J.; König, B. Decarboxylative Reactions with and without Light – a Comparison.

Green Chem. **2018**, *20* (2), 323–361. https://doi.org/10.1039/C7GC02949G.

(6) Beil, S. B.; Chen, T. Q.; Intermaggio, N. E.; Macmillan, D. W. C. Carboxylic Acids as Adaptive Functional Groups in Metallaphotoredox Catalysis. *Acc. Chem. Res.* **2022**, *55* (23), 3481–3494. https://doi.org/10.1021/acs.accounts.2c00607.

(7) Arias-Rotondo, D. M.; McCusker, J. K. The Photophysics of Photoredox Catalysis: A Roadmap for Catalyst Design. *Chem. Soc. Rev.* **2016**, *45* (21), 5803–5820. https://doi.org/10.1039/C6CS00526H.

(8) Rehm, D.; Weller, A. Kinetics of Fluorescence Quenching by Electron and H-Atom Transfer. *Isr. J. Chem.* **1970**, *8* (2), 259–271. https://doi.org/10.1002/ijch.197000029.

(9) Marcus, R. A. Electron Transfer Reactions in Chemistry: Theory and Experiment (Nobel Lecture). *Angew. Chem., Int. Ed.* **1993**, *32* (8), 1111–1121. https://doi.org/10.1002/anie.199311113.

(10) López, S. E.; Salazar, J. Trifluoroacetic Acid: Uses and Recent Applications in Organic Synthesis. *J. Fluor. Chem.* **2013**, *156*, 73–100. https://doi.org/10.1016/j.jfluchem.2013.09.004.

(11) Li, H.-P.; He, X.-H.; Peng, C.; Li, J.-L.; Han, B. A Straightforward Access to Trifluoromethylated Natural Products through Late-Stage Functionalization. *Nat. Prod. Rep.* **2022**, *39*, 1111–1368. https://doi.org/10.1039/D2NP00056C.

(12) Najardarson, J. T. Top 200 Small Molecule Pharmaceuticals by Retail Sales in 2021 https://njardarson.lab.arizona.edu/sites/njardarson.lab.arizona.edu/files/Top 200 Small Molecules 2021V3.pdf.

(13) Baguia, H.; Evano, G. Direct Perfluoroalkylation of C−H Bonds in (Hetero)Arenes. *Chem. – A Eur. J.* **2022**, *28* (41). https://doi.org/10.1002/chem.202200975.

(14) Depecker, C.; Marzouk, H.; Trevin, S.; Devynck, J. Trifluoromethylation of Aromatic Compounds via Kolbe Electrolysis in Pure Organic Solvent. Study on Laboratory and Pilot Scale. *New J. Chem.* **1999**, *23* (7), 739–742. https://doi.org/10.1039/a901305i.

(15) Tanabe, Y.; Matsuo, N.; Ohno, N. Direct Perfluoroalkylation Including Trifluoromethylation of Aromatics with Perfluoro Carboxylic Acids Mediated by Xenon Difluoride. *J. Org. Chem.* **1988**, *53* (19), 4582–4585. https://doi.org/10.1021/jo00254a033.

(16) Sawada, H.; Nakayama, M.; Yoshida, M.; Yoshida, T.; Kamigata, N. Trifluoromethylation of Aromatic Compounds with Bis(Trifluoroacetyl) Peroxide. *J. Fluor. Chem.* **1990**, *46* (3), 423–431. https://doi.org/10.1016/S0022-1139(00)82927-9.

(17) Hilborn, J. W.; Pincock, J. A. Rates of Decarboxylation of Acyloxy Radicals Formed In the Photocleavage of Substituted 1-Naphthylmethyl Alkanoates. *J. Am. Chem. Soc.* **1991**, *113* (7), 2683–2686. https://doi.org/10.1021/ja00007a049.

(18) Rijs, N. J.; O'Hair, R. A. J. Forming Trifluoromethylmetallates: Competition between Decarboxylation and C–F Bond Activation of Group 11 Trifluoroacetate Complexes, [CF3CO2ML]−. *Dalt. Trans.* **2012**, *41* (12), 3395. https://doi.org/10.1039/c2dt12117d.

(19) Li, Y.; Chen, T.; Wang, H.; Zhang, R.; Jin, K.; Wang, X.; Duan, C. A Ligand-Free Copper-Catalyzed Decarboxylative Trifluoromethylation of Aryliodides with Sodium Trifluoroacetate Using Ag2O as a Promoter. *Synlett* **2011**, *2011* (12), 1713–1716. https://doi.org/10.1055/s-0030-1260930.

(20) McReynolds, K. A.; Lewis, R. S.; Ackerman, L. K. G.; Dubinina, G. G.; Brennessel, W. W.; Vicic, D. A. Decarboxylative Trifluoromethylation of Aryl Halides Using Well-Defined

13

Copper-Trifluoroacetate and -Chlorodifluoroacetate Precursors. *J. Fluor. Chem.* **2010**, *131* (11), 1108–1112. https://doi.org/10.1016/j.jfluchem.2010.04.005.

(21) Chen, M.; Buchwald, S. L. Rapid and Efficient Trifluoromethylation of Aromatic and Heteroaromatic Compounds Using Potassium Trifluoroacetate Enabled by a Flow System. *Angew. Chem., Int. Ed.* **2013**, *52* (44), 11628–11631. https://doi.org/10.1002/anie.201306094.

(22) Shi, G.; Shao, C.; Pan, S.; Yu, J.; Zhang, Y. Silver-Catalyzed C-H Trifluoromethylation of Arenes Using Trifluoroacetic Acid as the Trifluoromethylating Reagent. *Org. Lett.* **2015**, *17* (1), 38–41. https://doi.org/10.1021/ol503189j.

(23) Exner, B.; Bayarmagnai, B.; Jia, F.; Goossen, L. J. Iron-Catalyzed Decarboxylation of Trifluoroacetate and Its Application to the Synthesis of Trifluoromethyl Thioethers. *Chem. - A Eur. J.* **2015**, *21* (48), 17220–17223. https://doi.org/10.1002/chem.201503915.

(24) Lai, C.; Mallouk, T. E. A New Approach to the Photochemical Trifluoromethylation of Aromatic Compounds. *J. Chem. Soc. Chem. Commun.* **1993**, No. 17, 1359–1361. https://doi.org/10.1039/C39930001359.

(25) Bazyar, Z.; Hosseini-Sarvari, M. Au@ZnO Core-Shell: Scalable Photocatalytic Trifluoromethylation Using CF3CO2Na as an Inexpensive Reagent under Visible Light Irradiation. *Org. Process Res. Dev.* **2019**, *23* (11), 2345–2353. https://doi.org/10.1021/acs.oprd.9b00225.

(26) Lin, J.; Li, Z.; Kan, J.; Huang, S.; Su, W.; Li, Y. Photo-Driven Redox-Neutral Decarboxylative Carbon-Hydrogen Trifluoromethylation of (Hetero)Arenes with Trifluoroacetic Acid. *Nat. Commun.* **2017**, *8*, 1–7. https://doi.org/10.1038/ncomms14353.

(27) Beatty, J. W.; Douglas, J. J.; Cole, K. P.; Stephenson, C. R. J. A Scalable and Operationally Simple Radical Trifluoromethylation. *Nat. Commun.* **2015**, *6* (1), 7919. https://doi.org/10.1038/ncomms8919.

(28) Yin, D.; Su, D.; Jin, J. Photoredox Catalytic Trifluoromethylation and Perfluoroalkylation of Arenes Using Trifluoroacetic and Related Carboxylic Acids. *Cell Reports Phys. Sci.* **2020**, *1* (8), 100141. https://doi.org/10.1016/j.xcrp.2020.100141.

(29) Zhang, M.; Chen, J.; Huang, S.; Xu, B.; Lin, J.; Su, W. Photocatalytic Fluoroalkylations of (Hetero)Arenes Enabled by the Acid-Triggered Reactivity Umpolung of Acetoxime Esters. *Chem Catal.* **2022**, *2* (7), 1793–1806. https://doi.org/10.1016/j.checat.2022.05.018.

(30) Abderrazak, Y.; Bhattacharyya, A.; Reiser, O. Visible-Light-Induced Homolysis of Earth-Abundant Metal-Substrate Complexes: A Complementary Activation Strategy in Photoredox Catalysis. *Angew. Chem., Int. Ed.* **2021**, *60* (39), 21100–21115. https://doi.org/10.1002/anie.202100270.

(31) Juliá, F. Ligand-to-Metal Charge Transfer (LMCT) Photochemistry at 3d-Metal Complexes: An Emerging Tool for Sustainable Organic Synthesis. *ChemCatChem* **2022**, *14* (19). https://doi.org/10.1002/cctc.202200916.

(32) Sugimori, A.; Yamada, T. Visible Light- and Radiation-Induced Alkylation of Pyridine Ring with Alkanoic Acid. Effective Alkylation in the Presence of Iron(III) Sulfate. *Bull. Chem. Soc. Jpn.* **1986**, *59*, 3911–3915.

(33) Poznyak, A. L.; Pavlovski, V. I. Photochemical Reactions of Ligands in Transition-Metal Complexes. *Angew. Chem., Int. Ed.* **1988**, *27* (6), 789–796. https://doi.org/10.1002/anie.198807891.

(34) Reichle, A.; Sterzel, H.; Kreitmeier, P.; Fayad, R.; Castellano, F. N.; Rehbein, J.; Reiser, O.

Copper(Ii)-Photocatalyzed Decarboxylative Oxygenation of Carboxylic Acids. *Chem. Commun.* **2022**, *58* (28), 4456–4459. https://doi.org/10.1039/d2cc00570k.

(35) Li, Q. Y.; Gockel, S. N.; Lutovsky, G. A.; DeGlopper, K. S.; Baldwin, N. J.; Bundesmann, M. W.; Tucker, J. W.; Bagley, S. W.; Yoon, T. P. Decarboxylative Cross-Nucleophile Coupling via Ligand-to-Metal Charge Transfer Photoexcitation of Cu(Ii) Carboxylates. *Nat. Chem.* **2022**, *14* (1), 94–99. https://doi.org/10.1038/s41557-021-00834-8.

(36) Xu, P.; Su, W.; Ritter, T. Decarboxylative Sulfoximination of Benzoic Acids Enabled by Photoinduced Ligand-to-Copper Charge Transfer. *Chem. Sci.* **2022**, *13* (45), 13611–13616. https://doi.org/10.1039/D2SC05442F.

(37) Xu, P.; López-Rojas, P.; Ritter, T. Radical Decarboxylative Carbometalation of Benzoic Acids: A Solution to Aromatic Decarboxylative Fluorination. *J. Am. Chem. Soc.* **2021**, *143* (14), 5349–5354. https://doi.org/10.1021/jacs.1c02490.

(38) Dow, N. W.; Pedersen, P. S.; Chen, T. Q.; Blakemore, D. C.; Dechert-Schmitt, A. M.; Knauber, T.; Macmillan, D. W. C. Decarboxylative Borylation and Cross-Coupling of (Hetero)Aryl Acids Enabled by Copper Charge Transfer Catalysis. *J. Am. Chem. Soc.* **2022**, *144* (14), 6163–6172. https://doi.org/10.1021/jacs.2c01630.

(39) Chen, T. Q.; Pedersen, P. S.; Dow, N. W.; Fayad, R.; Hauke, C. E.; Rosko, M. C.; Danilov, E. O.; Blakemore, D. C.; Dechert-Schmitt, A.-M.; Knauber, T.; Castellano, F. N.; MacMillan, D. W. C. A Unified Approach to Decarboxylative Halogenation of (Hetero)Aryl Carboxylic Acids. *J. Am. Chem. Soc.* **2022**, *144* (18), 8296–8305. https://doi.org/10.1021/jacs.2c02392.

(40) Lu, Y.; West, J. G. Chemoselective Decarboxylative Protonation Enabled by Cooperative Earth-Abundant Element Catalysis. *Angew. Chem., Int. Ed.* **2022**, *62* (3). https://doi.org/10.1002/anie.202213055.

(41) Li, Z.; Wang, X.; Xia, S.; Jin, J. Ligand-Accelerated Iron Photocatalysis Enabling Decarboxylative Alkylation of Heteroarenes. *Org. Lett.* **2019**, *21* (11), 4259–4265. https://doi.org/10.1021/acs.orglett.9b01439.

(42) Kao, S.-C.; Bian, K.-J.; Chen, X.-W.; Chen, Y.; Martí, A. A.; West, J. G. Photochemical Iron-Catalyzed Decarboxylative Azidation via the Merger of Ligand-to-Metal Charge Transfer and Radical Ligand Transfer Catalysis. *Chem Catal.* **2023**, *3* (6), 100603. https://doi.org/10.1016/j.checat.2023.100603.

(43) Feng, G.; Wang, X.; Jin, J. Decarboxylative C-C and C-N Bond Formation by Ligand-Accelerated Iron Photocatalysis. *European J. Org. Chem.* **2019**, *2019* (39), 6728–6732. https://doi.org/10.1002/ejoc.201901381.

(44) Wang, Y.; Li, L.; Fu, N. Electrophotochemical Decarboxylative Azidation of Aliphatic Carboxylic Acids. *ACS Catal.* **2022**, *12* (17), 10661–10667. https://doi.org/10.1021/acscatal.2c02934.

(45) Shirase, S.; Tamaki, S.; Shinohara, K.; Hirosawa, K.; Tsurugi, H.; Satoh, T.; Mashima, K. Cerium(IV) Carboxylate Photocatalyst for Catalytic Radical Formation from Carboxylic Acids: Decarboxylative Oxygenation of Aliphatic Carboxylic Acids and Lactonization of Aromatic Carboxylic Acids. *J. Am. Chem. Soc.* **2020**, *142* (12), 5668–5675. https://doi.org/10.1021/jacs.9b12918.

(46) Yatham, V. R.; Bellotti, P.; König, B. Decarboxylative Hydrazination of Unactivated Carboxylic Acids by Cerium Photocatalysis. *Chem. Commun.* **2019**, *55* (24), 3489–3492. https://doi.org/10.1039/C9CC00492K.

(47) See Supporting Information for Details.

(48) Nagib, D. A.; Macmillan, D. W. C. Trifluoromethylation of Arenes and Heteroarenes by Means of Photoredox Catalysis. *Nature* **2011**, *480* (7376), 224–228. https://doi.org/10.1038/nature10647.

(49) Dorababu, A. Indole-a Promising Pharmacophore in Recent Antiviral Drug Discovery. *RSC Med. Chem.* **2020**, *11* (12), 1335–1353. https://doi.org/10.1039/d0md00288g.

(50) Mejía, E.; Togni, A. Rhenium-Catalyzed Trifluoromethylation of Arenes and Heteroarenes by Hypervalent Iodine Reagents. *ACS Catal.* **2012**, *2* (4), 521–527. https://doi.org/10.1021/cs300089y.

(51) Akiyama, T.; Kato, K.; Kajitani, M.; Sakaguchi, Y.; Nakamura, J.; Hayashi, H.; Sugimori, A. Photochemical Trifluoromethylation of Some Aromatic and Heteroaromatic Compounds with Trifluoromethyl Bromide. *Bull. Chem. Soc. Jpn.* **1988**, *61* (10), 3531–3537. https://doi.org/10.1246/bcsj.61.3531.

(52) Ji, Y.; Brueckl, T.; Baxter, R. D.; Fujiwara, Y.; Seiple, I. B.; Su, S.; Blackmond, D. G.; Baran, P. S. Innate C-H Trifluoromethylation of Heterocycles. *Proc. Natl. Acad. Sci. U. S. A.* **2011**, *108* (35), 14411–14415. https://doi.org/10.1073/pnas.1109059108.

(53) O'Hara, F.; Blackmond, D. G.; Baran, P. S. Radical-Based Regioselective C-H Functionalization of Electron-Deficient Heteroarenes: Scope, Tunability, and Predictability. *J. Am. Chem. Soc.* **2013**, *135* (32), 12122–12134. https://doi.org/10.1021/ja406223k.

(54) Langlois, B. R.; Laurent, E.; Roidot, N. Trifluoromethylation of Aromatic Compounds with Sodium Trifluoromethanesulfinate under Oxidative Conditions. *Tetrahedron Lett.* **1991**, *32* (51), 7525–7528. https://doi.org/10.1016/0040-4039(91)80524-A.

(55) Ham, W. S.; Hillenbrand, J.; Jacq, J.; Genicot, C.; Ritter, T. Divergent Late-Stage (Hetero)Aryl C−H Amination by the Pyridinium Radical Cation. *Angew. Chem., Int. Ed.* **2019**, *58* (2), 532–536. https://doi.org/10.1002/anie.201810262.